A TECHNIQUE OF EVALUATING FUEL LOSSES DUE TO METEOROID PUNCTURE AND SOME TIMELY EXAMPLES[1]

Andrew H. Jazwinski[2]

Martin Company, Baltimore 3, Maryland

ABSTRACT

An important hazard to which space vehicles are exposed is loss of fuel due to meteoroid puncture of fuel tanks. The meteoroid spectrum of significance here is poorly defined, since satellite measurements--to date--have dealt with meteoroids of considerably smaller mass than those of interest. Visual, photographic and radio-radar data do not yield mass directly. A conservative meteoroid environment is defined. With the aid of a hypervelocity penetration relation (18),[3] a hole production model is introduced--and methods are presented for calculating fuel losses as a function of time and probability. Two space missions are analyzed as examples: 1) Earth-Moon transfer of a liquid hydrogen fuel tank to be used for Earth-return, and 2) storage of a similar fuel tank in an Earth-parking orbit for later rendezvous. Tank skins of steel and aluminum are considered, with equivalent tank skin thickness as a parameter. It is found that fuel losses may indeed be significant and that means should be taken to limit or eliminate them by shielding the fuel tanks.

INTRODUCTION

The advent of space exploration has stimulated interest in the meteoroid environment and its effects on space vehicles. Kornhauser (1) calculated hole area produced and pressure

Presented at the ARS Lunar Missions Meeting, Cleveland, Ohio, July 17-19, 1962.

[1] Research conducted at General Dynamics/Astronautics, San Diego, California.

[2] Senior Engineer, Aero-Space Mechanics Department.

[3] Numbers in parentheses indicate References at end of paper.

losses vs time at various probability levels, assuming an average conservative situation. Bjork (2) estimated steel and aluminum armor weights required to protect a vehicle at any confidence level. The author (3-5) estimated conservative fuel losses on the Centaur vehicle, using at first an approximate probabilistic approach. More recently Edmiston (6) developed relations for the meteoroid hole area produced as a function of time and probability, based on two penetration models.

Four distinct problem areas exist in evaluating fuel losses due to meteoroid puncture. They are 1) properties of the meteoroid environment which the vehicle traverses, 2) the penetration process whereby holes are produced in the vehicle, 3) flow relations for the escaping fuel, and 4) probabilistic evaluation of the fuel losses. These problems are discussed in the sequel.

The vehicle designer wishes to know the average or mean effect of the meteoroid environment on his vehicle, as well as to have some measure of the dispersion from this mean--i.e., that effect which will not be exceeded at some high probability. Both effects are presented here. The analysis is applied to two specific cases: 1) A fuel tank transported to the Moon to be used for Earth-return, and 2) a fuel storage tank in an Earth-parking orbit. Fuel losses are studied as a function of tank-skin thickness for aluminum and steel skins.

METEOROID ENVIRONMENT

Current knowledge of the meteoroid environment is very limited. Its properties of interest in relation to the present problem include meteoroid density, mass-flux, mass-velocity and spatial distributions. Ideally, it would be desirable to know the environmental parameters as a function of time and position in space. This is virtually impossible, because of the existence of meteoroid showers (7), as well as meteor showers (8)--in addition to the sporadic background. These have been known to exceed the sporadic background by several orders of magnitude. Only the sporadic meteoroid flux can be considered here.

Whipple (9) reports that more than 90% of all photographic meteors have densities as low as 0.05 gm/cm^3. Radio-radar meteors may have similar densities. This applies to meteors of mass roughly greater than 10^{-4} gm, commonly referred to as "dust balls." These dust balls may break up, however, producing smaller particles with more conventional densities,

perhaps more like those of silicate rocks.

The asteroids may be the source of a large fraction of the meteoroid spectrum of smaller masses ($<10^{-4}$ gm). Brown (10, 11) correlates the mass-frequency distribution of meteorites with that of the asteroids. The correlation is good. Meteorites range in density from 2.7 to 7.9 gm/cm^3 (stones-irons), the relative abundance being about 16 to 1, respectively. This would place the average density of asteroidal meteoroids at about 3 gm/cm^3.

In view of the uncertainty that is present, the fact that meteoroids of mass less than 10^{-4} gm may play a crucial role in contributing to fuel losses (as will be seen later) and of the desire for a conservative estimate of fuel losses, a density of 3 gm/cm^3 will be assumed for all meteoroids.

Geocentric velocities of meteors have been measured. Whipple (9) calculates the average velocity of photographic meteors to be 28 km/sec. A range of 11-72 km/sec is possible, since (9) meteors are permanent members of the solar system. One would expect smaller meteoroids to have lower velocities. On this basis, Whipple (9) constructed a table of velocity as a function of mass. This is plotted in Fig. 1 and represents the most reasonable velocity distribution which presently can be deducted. A conservative figure of 28 km/sec may be used for all meteoroids.

Data as to the flux of meteoroids have been obtained from visual, photographic and radio-radar observations--and of late from counting devices on rockets and satellites. Data in the first category (i.e., visual, photographic and radio-radar) yield meteor flux as a function of magnitude. It is then necessary to relate magnitude to the mass of the particle. To date, no reliable relation exists. Whipple (9) assigned a value of 25 gm to a zero magnitude meteor, while Watson (8) chose the value 0.25 gm. On these bases two curves are obtained of the flux of meteoroids of mass equal to and greater than mass m, as a function of mass. These have been extrapolated to particles of smaller mass (8, 9) and are shown in Fig. 2. The two estimates can, perhaps, be taken as bounds on the sporadic meteoroid environment in the mass range from 10^{-4} to 1 gm.

A rather complete list of in situ rocket and satellite measurements has been compiled by the author (5) and is

thoroughly referenced. The most significant measurements are presented in Fig. 2. They are listed in order of decreasing significance, the solid symbols representing the most significant measurements. The points plotted are based on an assumed velocity of 15 km/sec, since satellite sensors respond to momentum[4]. The data have not been corrected for Earth-shielding, as is sometimes the custom (12), since, while in Earth's vicinity, a vehicle will see the shielded flux and there are theoretical indications (13-15) that flux decreases with increasing altitude.

The most significant measurements have reportedly (12) been taken on the Explorer VIII satellite, where measurements were made in three momentum ranges. The three Explorer VIII points fall on a good straight line, marked "Direct" in Fig. 2, which also fits the other satellite data rather well. This line may be taken, at present, as the best representation of the sporadic meteoroid environment in the mass range from 10^{-9} to 10^{-6} gm. A closer inspection of the satellite data (5, 12) indicates that no altitude dependence of the flux is discernible. The mean altitudes of the satellite orbits vary, at most, by 800 km (5)--and the rocket data cannot be considered significant.

At the present time, then, no altitude dependence can be deduced experimentally and, therefore, it will be assumed that meteoroid flux is Earth-distance independent in cislunar space.

It can be seen that no measurements of meteoroid flux are available in the mass range from 10^{-6} to 10^{-4} or 10^{-3} gm. This, as will be seen, is unfortunately the most important mass regime as far as fuel losses due to puncture are concerned. Sensor surfaces have been very small in the past, because of the weight limitation. Hence, they have had to be of high sensitivity to record a significant number of hits.

Consequently, a conservative mass-flux relation has to be estimated. It is believed that Whipple's curve (Fig. 2) represents such a relation. Meteoroid flux, therefore, will be assumed to follow the law

$$\phi = 10^{-12.2}\, m^{-1.0} \qquad [1]$$

where m is the meteoroid mass in grams and ϕ is the number

[4]Russian sensors reportedly respond to the kinetic energy of the impacting particle.

of particles of mass greater than and equal to m per m^2-sec.

A more complete discussion of meteoroid flux is given in Refs. 5 and 3.

HOLE AREA DUE TO METEOROID PUNCTURE

Meteoroid puncture of a vehicle tank skin involves a hypervelocity impact process which of late has received considerable attention. An excellent compilation and analysis of experimental and theoretical work is presented by Herrmann and Jones (16). Until recently, velocities attained in the laboratory have not exceeded 6 km/sec. Some shots at velocities up to 12 km/sec have been obtained (17). As can be seen, meteoroid velocities have barely been approached in the laboratory. Extrapolation of these experimental data taken at low velocities to the much higher meteoroid velocities is strictly invalid (5, 16), since the physical process involved is different. At hypervelocities, strength effects are negligible (16, 18) during part of the impact process, because the pressures involved far exceed the material strength.

The most applicable theoretical work appears to be that of Bjork (18), who solved the equations for a hydrodynamic impact of iron on iron and aluminum on aluminum numerically in the inviscid, adiabatic approximation. He obtained the relations

$$\text{Al on Al:} \quad p = 1.09\,(mv)^{1/3} \qquad [2]$$

$$\text{Fe on Fe:} \quad p = 0.606\,(mv)^{1/3}$$

where p is the depth of penetration in a semi-infinite target in cm, m is the meteoroid mass in gm, and v is the meteoroid velocity in km/sec.

Bjork (19) recently suggested that the penetration in a given target material by projectiles of different materials having the same mass and velocity is proportional to the initial interface velocity on impact. Herrmann and Jones (16) show that initial interface velocities v* for impacts of dissimilar materials are given with a maximum error of about 20% for most materials by

$$v^* = (\rho_p/\rho_t)^{1/3}\, v/2 \qquad [3]$$

for projectile velocities v above 3 km/sec, where ρ_p and ρ_t

are projectile and target densities, respectively.

Equation 2, therefore, can be modified for different projectile materials to yield

$$p = 1.09 (\rho_p/\rho_{Al})^{1/3} (mv)^{1/3} \quad [4]$$

for impacts on aluminum targets, and

$$p = 0.606 (\rho_p/\rho_{Fe})^{1/3} (mv)^{1/3} \quad [5]$$

for impacts on iron targets.

It has been observed (16) that, if a projectile will penetrate a semi-infinite target to a depth of p, it will puncture a thin plate of thickness 1.5 p. Therefore, in terms of plate thickness, Eqs.4 and 5 become

$$t_{Al} = 1.64 (\rho_p/\rho_{Al})^{1/3} (mv)^{1/3} \quad [6]$$

$$t_{Fe} = 0.908 (\rho_p/\rho_{Fe})^{1/3} (mv)^{1/3}. \quad [7]$$

These relations will be used in further analysis.

Equations 6 and 7 may be combined with Eq.1 to yield the flux of meteoroids which will puncture a thin vehicle skin of thickness t. This will be called, after Bjork (2), the penetrating flux ψ. Given a skin thickness t, and taking velocities from Fig. 1, or assuming a meteoroid velocity of 28 km/sec, Eqs. 6 and 7 yield the smallest mass meteoroids which will puncture the skin. This will be called the threshold mass m_t.

All meteoroids of mass greater than m_t will likewise puncture the skin. Using velocities from Fig. 1 and meteoroid density $\rho_m = \rho_p = 3$ gm/cm^3, m_t was calculated as a function of skin thickness for both steel and aluminum skins and appears in Fig. 3. It is seen that meteoroids of mass as low as 10^{-6} gm may be important in contributing to fuel losses.

It will be assumed that the hole produced by a meteoroid impact is of constant diameter throughout its depth, the diameter being equal to the entrance diameter produced by the meteoroid. The depth of penetration p, given in Eqs. 4 and 5, is also the radius of the hole. Therefore, the area of a hole produced by a meteoroid of mass m is given by

$$a(m) = \pi p^2 = \pi C^2 (\rho_m/\rho_{Al \text{ or } Fe})^{2/3} [mv(m)]^{2/3} \quad [8]$$

where C = 1.09 for aluminum targets, C = 0.606 for steel targets, and ρ_m is the meteoroid density. For ρ_m = 3, Eq.8 is quite accurate for meteoroids of mass near the threshold mass, since the ratio of skin thickness to diameter of threshold meteoroid (assuming a spherical meteoroid) is 6 and 2.33 for aluminum and steel targets, respectively.

For meteoroids of mass greater than the threshold mass, Eq.8 will overestimate the actual area--the overestimate increasing as mass increases. This is because (16) the radius of a crater produced by a given projectile in a semi-infinite target is greater than the radius of a hole produced by the same projectile in a thin plate. Since the significance (i.e., number) of meteoroids decreases with increasing mass, above the threshold mass, the error introduced by using Eq.8 for all meteoroids will not be substantial. At any rate, Eq.8 gives a conservative estimate of area.

Hole area versus meteoroid mass for both aluminum and steel is given in Fig. 4.

FUEL FLOW

Fluid flow out of small orifices is currently not well understood. Bernoulli flow from a reservoir at zero-g into a vacuum will be used. The exhaust velocity is therefore given by

$$v_e = (2P/\rho_f)^{1/2} \quad [9]$$

where P is the tank pressure and ρ_f the fuel density. The flow rate is therefore

$$Q = r a (2P/\rho_f)^{1/2} \quad [10]$$

where r is an orifice coefficient and a the area. The mass flow rate is

$$Q_m = r a (2P\rho_f)^{1/2}. \quad [11]$$

When dealing with cryogenic liquids, the question may be raised whether the liquid might not freeze while expanding through the hole; thus temporarily plugging the hole and decreasing the effective flow rate. Each situation must be

examined independently for this effect.

MEAN FUEL LOSSES

A vehicle with tank area A, exposed to a penetrating flux ψ for a time τ will suffer an average number of punctures $\lambda = \psi A \tau$. The probability that a meteoroid in the mass range dm will puncture the tank skin is

$$-d\phi/\psi \qquad [12]$$

where $-d\phi$ is the number of meteoroids in dm. Now from Eq.1

$$-d\phi = (K/m^2)\, dm \qquad [13]$$

where $K = 10^{-12.2}$. Therefore,

$$-d\phi/\psi = \left(m_t/m^2\right)dm \qquad [14]$$

Of course, the total probability is

$$\int_{\psi}^{0} -d\phi/\psi = \int_{m_t}^{\infty} \left(m_t/m^2\right)dm = 1 \qquad [15]$$

The area of the average puncture is simply

$$A_e = \int_{m_t}^{\infty} \left(a(m)m_t/m^2\right)dm = \pi C^2 m_t \left(\rho_m/\rho_{Al\ or\ Fe}\right)^{2/3} \int_{m_t}^{\infty} \left(\left[m\, v(m)\right]^{2/3}/m^2\right) dm \qquad [16]$$

with the aid of Eq. 8. If the meteoroid velocity is a complicated function of mass, the integral in Eq. 16 is rather difficult. Assuming a constant velocity, $v(m) = V_o$ (28 km/sec), Eq. 16 is easily integrated

$$A_e = \frac{3\pi C^2}{3a_t} \left(\rho_m/\rho_{Al\ or\ Fe}\right)^{2/3} \left[m_t\, v_o\right]^{2/3} = \qquad [17]$$

where a_t is the area produced by the meteoroid of threshold mass.

In the average situation, then, the total hole area produced after time τ is $A_e\lambda = A_e \psi A\tau$, and the fuel losses at the end of the mission τ_T are

$$L_{AV} = (Q/a) \int_0^{\tau_T} A_e \psi A \tau \, d\tau = (Q/a) A_e \psi A \tau_T^2/2 =$$

$$(Q/a) A_e \lambda \tau_T/2 \qquad [18]$$

Equation 18 will be used subsequently in calculating average or mean fuel losses. The average area has been used in the past by the author (3,4) in calculating the approximate fuel losses at higher probabilities.

Meteoroids impacting a space vehicle constitute a random process developing in time (assuming that meteoroid flux is itself random) and, therefore, one would expect it to obey a Poisson distribution in the parameter λ. Lambda is also the mean of the Poisson distribution. Since the distribution is an asymmetric one, mean fuel losses are not the most probable losses; neither are they losses which will not be exceeded half the time--as is the case on a normal distribution. The Poisson distribution approximates a normal distribution for large λ (20), however, while departing from it radically for small λ.

FUEL LOSSES AT HIGHER PROBABILITIES

In theory, an infinite number of events may occur whereby the total area due to meteoroid punctures will not exceed a_T (as $a_T \to \infty$). There may be no punctures. There may be one puncture whose area does not exceed a_T. In general, there may be k punctures whose combined area does not exceed a_T, provided k is less than or equal to the integral part of a_T/a_t. If p_k is the probability of obtaining k punctures, and p'_k is the conditional probability that, given k punctures, their combined area will not exceed a_T, then the probability that the total hole area due to meteoroid punctures will not exceed a_T is

$$P(a_T) = \sum_{k=0}^{N} p_k \, p'_k \qquad [19]$$

where N is the integral part of a_T/a_t.

As discussed previously, it is reasonable to assume that the meteoroid flux obeys a Poisson distribution, i.e.,

$$p_k = e^{-\lambda} (\lambda^k / k!) \qquad [20]$$

Obviously,

$$p_1' = \int_{m_t}^{m(a_T)} \left(m_t / m^2\right) dm = (3/2)\, a_t^{3/2} \int_{a_t}^{a_T} a^{-5/2}\, da \qquad [21]$$

with the aid of Eq. 8, assuming $v(m) = V_o$ = constant, and

$$p_k' = \int_{a_t}^{a_T-(k-1)a_t} f(a_k)\, da_k \cdots \int_{a_t}^{a_T-a_t-a_3-\cdots-a_k} f(a_2)\, da_2 \int_{a_t}^{a_T-a_2-\cdots-a_k} f(a_1)\, da_1 \qquad [22]$$

where $f(a) = (3/2)\, a_t^{3/2}, a^{-5/2}$. These integrals become progressively more difficult as k increases.

Equation 22 has been derived by Edmiston (6). Although his penetration model was different, the functional dependence of area on mass was the same. In addition, he assumed a similar flux-mass relationship. His expression for p_k' is therefore exactly the same as Eq. 22, although a_t is obtained differently.

Equation 21 can be integrated readily, yielding

$$p_1' = 1 - (a_t / a_T)^{3/2} \qquad [23]$$

Edmiston (6) derived a lower bound formula for $p_k' (a_T/a_t)$ which results in a conservative estimate of a_T at any probability. This formula is

$$p_k' (a_T/a_t) \geq \left[p_1' (a_T / k\, a_t)\right]^k, \quad a_T/a_t \geq k \qquad [24]$$

With the aid of this expression, Eq. 19 may be written, for $a_T = na_t$

$$P(na_t) \simeq e^{-\lambda} \left\{ 1 + \sum_{k=1}^{n-1} \left(\lambda^k / k!\right) \left[1 - (k/n)^{3/2}\right]^k \right\}, \quad n = 1, 2, \ldots \qquad [25]$$

For any value of $P(na_t)$, Eq. 25 may be solved for $a_T = na_t$ as a function of λ. This has been done for $P(na_t) = 0.9986$ (3σ) and for $P(na_t) = 0.9772$ (2σ) and appears in Fig. 5. These curves may be fitted by polynomials in λ, yielding

$$a_T = a_t f(\lambda) = a_t f(\psi A \tau) \qquad [26]$$

The fuel losses, then, at the given probability $P(na_t)$ are given by

$$L_{P(na_t)} = \left(Q a_t / a\right) \int_{\tau_o}^{\tau_T} f(\psi A \tau) \, d\tau \qquad [27]$$

where the lower limit τ_o is the time corresponding to the λ value at which a_T begins to assume positive values as given in Fig. 5.

EARTH-MOON TRANSFER OF A FUEL TANK

A cylindrical fuel tank with 25 m^2 cylindrical exposed area might be used to transport liquid hydrogen to the moon to be used for Earth-return. Such a tank might hold approximately 2500 lb of fuel under pressure[5] of 23 psia. The density of liquid hydrogen is $\rho_f = 4.1$ lb/ft^3. An orifice coefficient of 0.6 is appropriate in this case. Transfer time will be taken to be 66 hours.

[5] Higher tank pressures might be used to prevent boiloff.

The question of whether plugging[6] may occur under these conditions might be asked. The author believes that plugging will not occur. The liquid will be out of the hole before it has a chance to freeze, in view of the very high exhaust velocities involved ($\sim 10^4$ cm/sec). Some pertinent experiments are now being conducted[7], including the measurement of orifice coefficients.

Mean, 2σ, and 3σ fuel losses were calculated as a function of skin thickness for both steel and aluminum skins. They appear in Figs. 6 and 7. It was assumed that the tank is an infinite reservoir for fuel; thus, losses are seen to exceed its capacity, which is approximately indicated.

An inspection of these figures reveals that 2σ and 3σ fuel losses become less than the mean losses for sufficiently thick skin. At first, this may be surprising. It means, however, that punctures become rare indeed and can occur only late in the mission, at a given probability. When they do occur, the hole area must be large--because the skin is thick. Therefore, they make a large contribution to mean losses, where--on the average--punctures may be thought of as occurring in the middle of the mission.

Moreover, 2σ and 3σ losses go to zero while mean losses remain finite. This is because, at the given probability, there are no punctures, while some still contribute to the mean. The rapid decrease of 2σ and 3σ losses is associated with the "jump" in area from zero to a_t observed in Fig. 5. There can be no hole unless its area is at least as large as that produced by a meteoroid of threshold mass.

Bjork (2) concluded that, weight for weight, aluminum skins are superior to steel skins because the penetrating flux, ψ, is lower. Figures 6 and 7 (as well as 8 and 9) exhibit this, in that the losses go to zero in agreement with

[6] Note added in proof: Preliminary visual observations at the General Dynamics/Astronautics Aerophysics Laboratory seem to indicate that no plugging occurs under the conditions described. High speed motion pictures revealed that intermittent plugging actually does take place. It is so rapid, however, that the orifice coefficient is not appreciably decreased unless the hole is extremely small. The value of 0.6, used here, appears to be reasonably good for the size holes under consideration. There are some indications that the orifice coefficient may be as high as 0.8 for the larger holes.

[7] General Dynamics/Astronautics Aerophysics Laboratory.

such a relation. When holes are allowed, however, the inverse is true. This is because, while weight for weight, the penetrating flux in aluminum skins is lower than in steel skins, the holes produced in aluminum are larger--the overall result being higher losses from an aluminum tank.

STORAGE TANK IN AN EARTH PARKING ORBIT

A liquid hydrogen fuel tank might be placed in an earth-parking orbit for later rendezvous. For the purpose of a numerical example, it will be assumed that the tank has an exposed cylindrical area of 50 m^2, capable of holding approximately 7000 lb of fuel. It is required that the tank remain in orbit for 30 days before rendezvous. Pressure, density and orifice coefficient will be taken to be the same as in the previous example. Mean, 2σ and 3σ fuel losses are given in Figs. 8 and 9 as a function of skin thickness for both steel and aluminum skins. Again, an infinite reservoir of fuel is assumed. Here, fuel losses are substantially higher than in the previous example, because mission time is considerably longer. Remarks similar to those in the previous example apply here.

CONCLUSIONS

A reasonably conservative estimate of the meteoroid environment was made and methods presented for the evaluation of fuel losses due to puncture of vehicle fuel tanks, resulting in conservative estimates of fuel losses. Fuel losses were studied as a function of tank skin thickness for steel and aluminum skins for two space missions. It was found that, weight for weight, a steel skin is superior to an aluminum skin for such thicknesses as allow punctures at a given probability. If such thicknesses are used as to exclude all punctures at a given probability, the inverse is true. Steel skins are always superior in terms of mean losses. The significance of mean losses is limited, however, when the average number of punctures is very small.

In general, fuel losses due to meteoroid puncture were found to be significant for single-skin tanks. Meteoroid shields should be considered as a means of reducing possible fuel losses. Weight for weight, thin, spaced skins have been found to be superior to single skins in reducing penetration by projectiles (16). If shields are used, the thicknesses discussed here may be thought of as "effective" skin thicknesses.

A comparison of fuel losses on the relatively short transfer mission (Figs. 6 and 7) with those in the relatively long parking orbit (Figs. 8 and 9) reveals that, although a tradeoff may exist between fuel lost and added weight of shielding for short missions, in general no such tradeoff exists for long ones. A puncture toward the beginning of a long mission may cause the loss of all fuel. Therefore, any meteoroid puncture during a long mission must be considered a "kill," and the vehicle must be shielded to eliminate all punctures at the desired probability.

The fuel losses presented here are conservative in another sense. As fuel is lost, the remaining fuel will assume a zero-gravity configuration. Some of the tank area will then be adjacent to empty space or, in the case of liquid hydrogen, to a gas ullage. The flow rate for hydrogen gas, under the conditions discussed, is about one-tenth of that for liquid hydrogen.

REFERENCES

1 Kornhauser, M., "Satellite pressure losses caused by meteoroid impacts," ARS J. 30, 475-479 (1960).

2 Bjork, R. L., "Meteoroids versus space vehicles," ARS J. 31, 803-807 (1961).

3 Jazwinski, A. H., "Fuel losses on a typical 6.2 hour Centaur mission due to meteoroid puncture," General Dynamics/Astronautics Rept. AE61-1042, August 1961.

4 Jazwinski, A. H., "Fuel losses on a typical 6.2 hour centaur mission due to meteoroid puncture, Addendum: "Variable Flight Time," General Dynamics/Astronautics Rept. AE61-1042 Addendum, December 12, 1961.

5 Jazwinski, A. H., "Meteoroid puncture of space vehicles with application to fuel losses on the centaur, General Dynamics/Astronautics Rept. AE62-0453, May 29, 1962.

6 Edmiston, R. M., "The production of a meteoroid hole area in a space vehicle near the Earth," Inst. Aerospace Sciences Paper No. 62-29, January 1962.

7 Dubin, M., Alexander, W. M., and Berg, O. E., "Cosmic dust showers by direct measurements," Symposium on the Astronomy and Physics of Meteors (1961).

8 Watson, F. G., Between the Planets, (Harvard University Press, Cambridge, Mass.) (1956), Chap. 7.

9 Whipple, F. L., "The meteoritic risk to space vehicles," Vistas in Astronautics, (1958).

10 Brown, Harrison, "The density of mass distribution of meteoritic bodies in the neighborhood of the earth's orbit," J. Geophys. Research 65, 1679 (June 1960).

11 Brown, Harrison, "Addendum: The density and mass distribution of meteoritic bodies in the neighborhood of the earth's orbit," J. Geophys. Research 66, 1316 (1961).

12 McCracken, C. W., and Alexander, W. M., "The distribution of small interplanetary dust particles in the vicinity of earth," Symposium on the Astronomy and Physics of Meteors (1961).

13 Beard, D. B., "Interplanetary dust distribution," Astrophys. Journal, 192, 496-506 (1959).

14 Singer, S. F., "Interplanetary dust near the earth," Nature 192, 321-323 (1961).

15 Whipple, F. L., "Particulate contents of space," Medical and Biological Aspects of the Energies of Space, Columbia University Press, New York (1961), Chap. 3.

16 Herrmann, W., and Jones, A. H., "Survey of hypervelocity impact information," Mass. Inst. Tech., ASRL Rept. No. 99-1, September 1961.

17 Eichelberger, R. L., and Gehring, J. W., "Effects of meteoroid impact on space vehicles," BRL Rept. No. 1155, December 1961.

18 Bjork, R. L., "Effects of a meteoroid impact on steel and aluminum in space," Xth International Astronautical Congress, London (1959).

19 Fifth Hypervelocity Impact Symposium, Denver (1961).

20 Feller, W., Probability Theory and Its Applications, John Wiley & Sons, Inc., London (1950), Chap. 7.

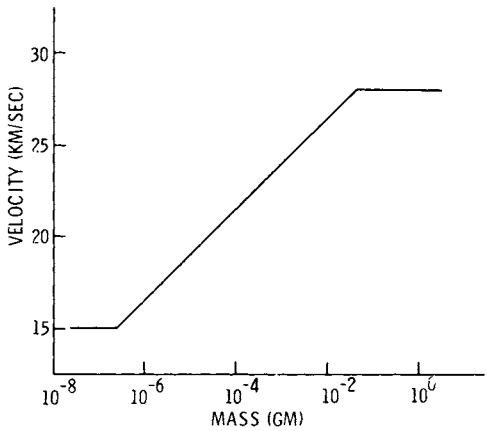

Fig. 1 Mass-velocity distribution of meteoroids after Whipple (9)

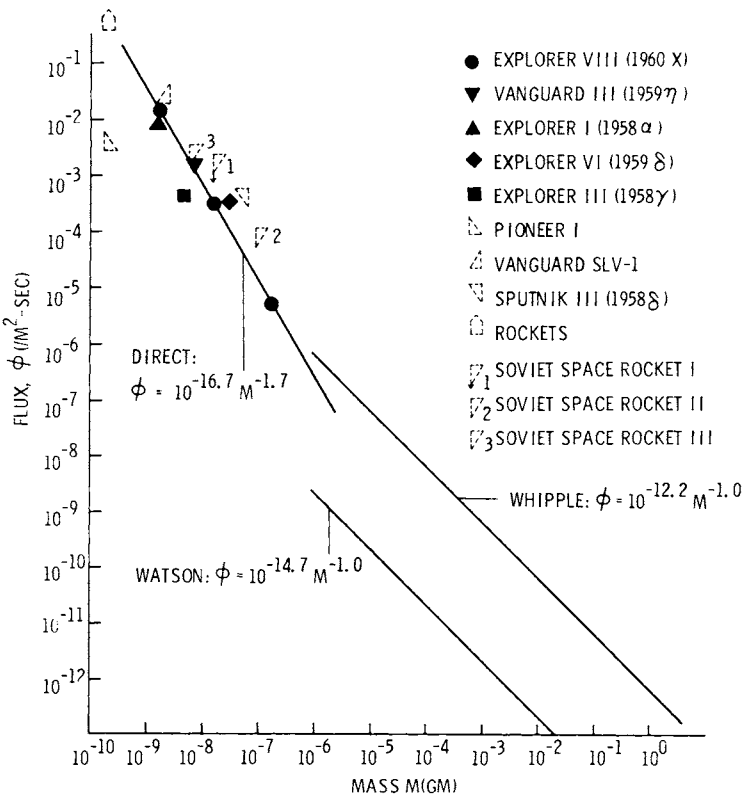

Fig. 2 Meteoroid flux

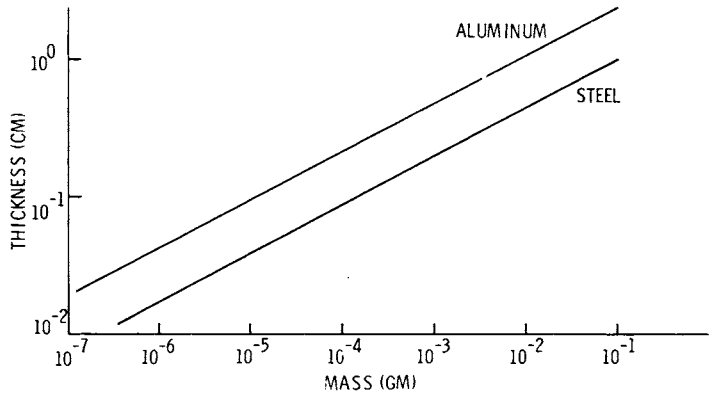

Fig. 3 Skin thickness versus threshold meteoroid mass

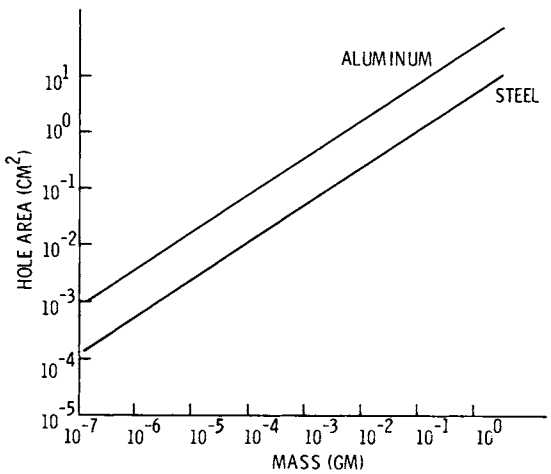

Fig. 4 Hole area versus meteoroid mass

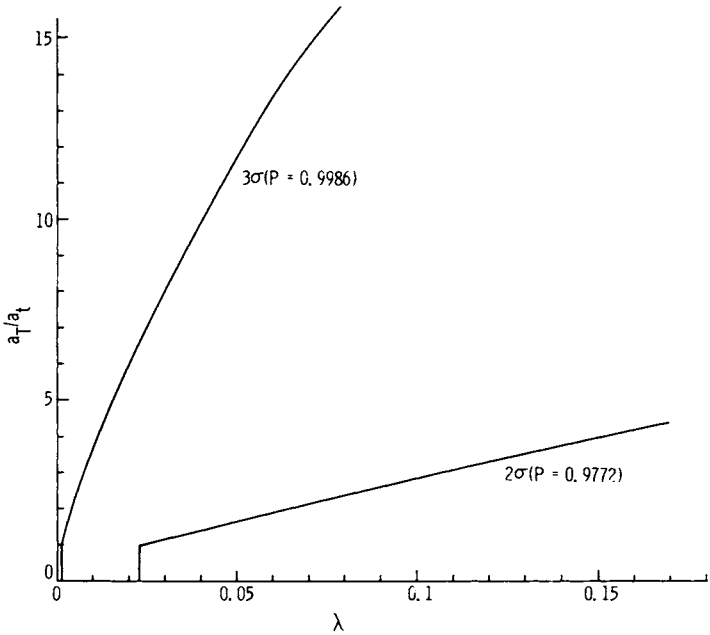

Fig. 5 Hole area as a function of time

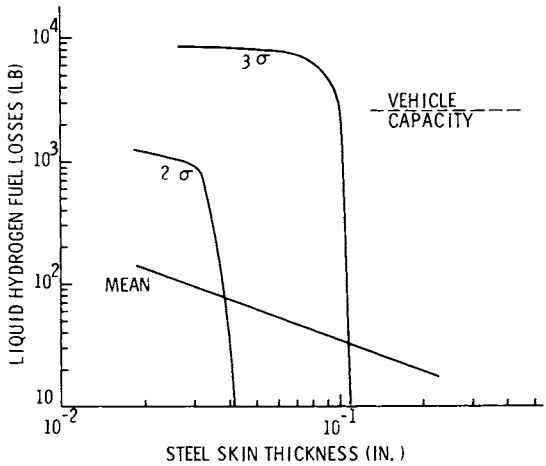

Fig. 6 Earth-moon transfer of steel fuel tank

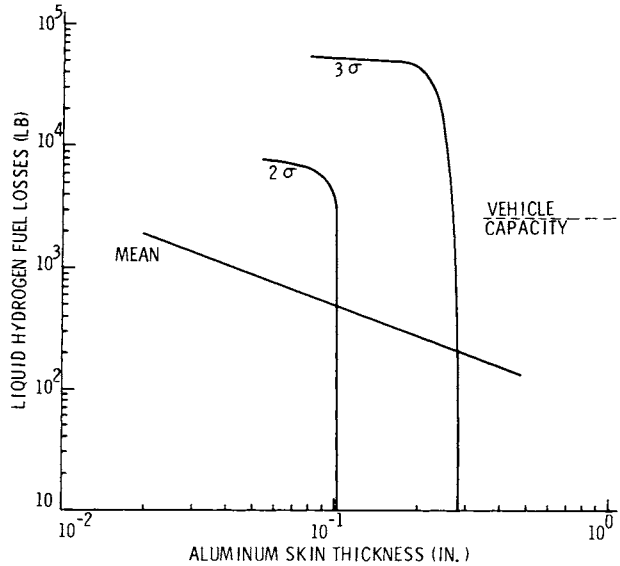

Fig. 7 Earth-moon transfer of aluminum fuel tank

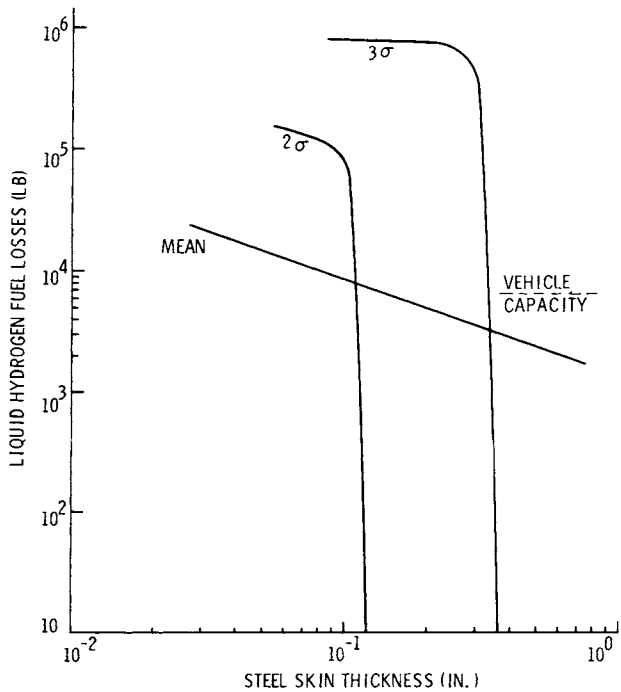

Fig. 8 Steel fuel storage tank in earth parking orbit

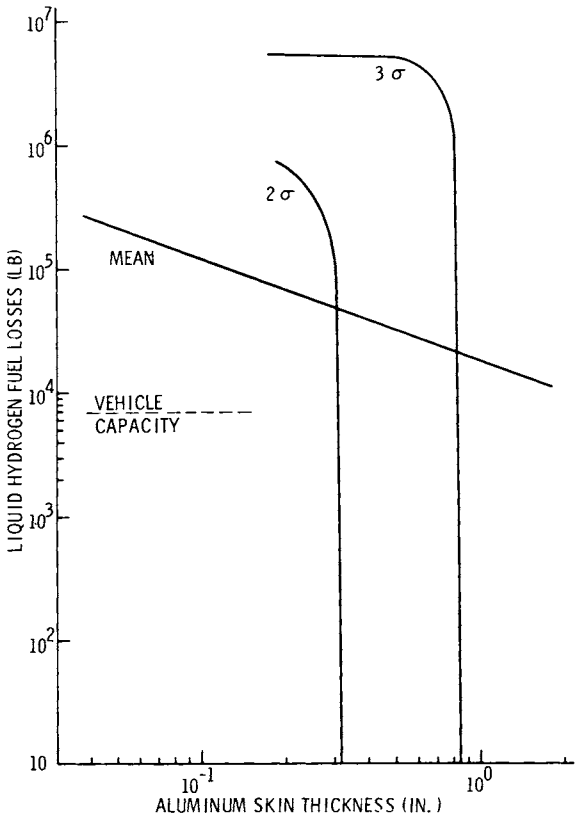

Fig. 9 Aluminum fuel storage tank in Earth parking orbit